Human Molecular Genetics, 2012, Vol. 21, No. 16 **3655–3667**
doi:10.1093/hmg/dds195
Advance Access published on May 28, 2012

Role of $Na_V1.9$ in activity-dependent axon growth in motoneurons

Narayan Subramanian[1,†,‡], Andrea Wetzel[1,†], Benjamin Dombert[1], Preeti Yadav[1], Steven Havlicek[1,¶], Sibylle Jablonka[1], Mohammed A. Nassar[2,§], Robert Blum[1,*,†] and Michael Sendtner[1,*,†]

[1]Institute for Clinical Neurobiology, University of Wuerzburg, Wuerzburg, Germany, and [2]Molecular Nociception Group, Wolfson Institute for Biomedical Research, University College London, London WC1E 6BT, UK

Received April 20, 2012; Revised and Accepted May 18, 2012

Spontaneous neural activity promotes axon growth in many types of developing neurons, including motoneurons. In motoneurons from a mouse model of spinal muscular atrophy (SMA), defects in axonal growth and presynaptic function correlate with a reduced frequency of spontaneous Ca^{2+} transients in axons which are mediated by N-type Ca^{2+} channels. To characterize the mechanisms that initiate spontaneous Ca^{2+} transients, we investigated the role of voltage-gated sodium channels (VGSCs). We found that low concentrations of the VGSC inhibitors tetrodotoxin (TTX) and saxitoxin (STX) reduce the rate of axon growth in cultured embryonic mouse motoneurons without affecting their survival. STX was 5- to 10-fold more potent than TTX and Ca^{2+} imaging confirmed that low concentrations of STX strongly reduce the frequency of spontaneous Ca^{2+} transients in somatic and axonal regions. These findings suggest that the $Na_V1.9$, a VGSC that opens at low thresholds, could act upstream of spontaneous Ca^{2+} transients. qPCR from cultured and laser-microdissected spinal cord motoneurons revealed abundant expression of $Na_V1.9$. $Na_V1.9$ protein is preferentially localized in axons and growth cones. Suppression of $Na_V1.9$ expression reduced axon elongation. Motoneurons from $Na_V1.9^{-/-}$ mice showed the reduced axon growth in combination with reduced spontaneous Ca^{2+} transients in the soma and axon terminals. Thus, $Na_V1.9$ function appears to be essential for activity-dependent axon growth, acting upstream of spontaneous Ca^{2+} elevation through voltage-gated calcium channels (VGCCs). $Na_V1.9$ activation could therefore serve as a target for modulating axonal regeneration in motoneuron diseases such as SMA in which presynaptic activity of VGCCs is reduced.

INTRODUCTION

Axons of developing motoneurons grow long distances before they make synaptic contacts with their target tissue, the skeletal muscle (1). During this period, motoneurons depend on neurotrophic factors for their survival (2–4). Cultured embryonic motoneurons also need neurotrophic factors for survival and neurite growth, thus allowing the analysis of signaling pathways for axon elongation and differentiation of presynaptic structures within axonal growth cones (1,5–7). Embryonic motoneurons exhibit spontaneous activity at early stages, before they make synaptic contact with skeletal muscles (8–12). Spontaneous Ca^{2+} elevation is an evolutionary conserved phenomenon in growth and differentiation of neurons (10,11,13–16) and is also observed in cultured mouse motoneurons (17). In motoneurons, spontaneous Ca^{2+} transients in axons and axonal growth cones contribute to axon extension and presynaptic differentiation (17). These characteristics are

*To whom correspondence should be addressed at: Institute for Clinical Neurobiology, University of Wuerzburg, Building E4, Versbacherstr. 5, 97078 Wuerzburg, Germany. Tel: +49 93120144001; Fax: +49 93120144001; Email: sendtner_m@klinik.uni-wuerzburg.de; blum_r@klinik.uni-wuerzburg.de
†These authors contributed equally to the work.
‡Present address: University of Medicine and Dentistry, Department of Neuroscience and Cell Biology, UMDNJ-Robert Wood Johnson Medical School, Piscataway, NJ 08854, USA.
¶Present address: Interdisciplinary Centre for Clinical Research, Nikolaus-Fiebiger Centre for Molecular Medicine, University Hospital Erlangen, 91054 Erlangen, Germany.
§Present address: Biomedical Science, University of Sheffield, Sheffield S10 2TN, UK.

also pathophysiologically relevant. Spontaneous Ca^{2+} transients are reduced in motoneurons from a mouse model of spinal muscular atrophy (SMA) (17), the predominant form of motoneuron disease in children and young adults. The reduced frequency of Ca^{2+} transients correlates with a reduced axon elongation and defective presynaptic differentiation *in vitro* (17), and disturbed synaptic transmission *in vivo* (18–20).

Survival and axon elongation of cultured motoneurons are strongly influenced by the availability of extracellular matrix proteins (1,21). Laminin-111 supports axon elongation in cultured motoneurons, while laminin-211/221 preparations reduce axon elongation (17). The synapse-specific β2-chain in laminin-221 mediates differentiation of presynaptic active zones by the direct interaction with $Ca_V2.2$, an N-type voltage-gated calcium channel (VGCC) (22). In *Smn*$^{-/-}$/*SMN2* mice, defects in the clustering of the $Ca_V2.2$ are observed in axon terminals (17).

We investigated the role of voltage-gated sodium channels (VGSCs) in activity-dependent axon elongation in cultured motoneurons and found that TTX and STX, specific pore-blockers of VGSCs, reduce spontaneous Ca^{2+} transients and also axon growth. High sensitivity to STX indicated that $Na_V1.9$ might contribute to spontaneous excitability in embryonic motoneurons. Indeed, motoneurons from $Na_V1.9$ knockout mice have shorter axons, and exhibit a reduced frequency of spontaneous Ca^{2+} transients. Taken together, these data indicate that $Na_V1.9$ plays a central role for spontaneous excitability that regulates the axonal growth in developing motoneurons.

RESULTS

VGSCs modulate axon growth in cultured motoneurons

To investigate whether VGSCs are involved in activity-dependent axon elongation, we tested the effects of the sodium-channel inhibitors tetrodotoxin (TTX) and saxitoxin (STX) in cultures of isolated spinal motoneurons. TTX binds all channels of the Na_V1-family with high affinity, except the TTX-insensitive channels (23). The TTX-insensitive channels $Na_V1.8$ and $Na_V1.9$ carry a serine (S) residue, whereas $Na_V1.5$ carries a cysteine residue in a critical TTX affinity motif, which is close to the selectivity determining (inner ring residues Asp, Glu, Lys, and Ala) motif of VGSCs (23–25). All other Na_V1-family members carry a phenylalanine (F) or tyrosine (Y) residue at the homologous site of domain DI, SS2-segment of the α-subunit (23,24). The determination of the equilibrium binding free energy of TTX and STX in dependence of these critical residues suggested that non-aromatic residues at the outer pore binding site of the channel shift the affinity of TTX-binding to lower values, while STX affinity is less affected (25).

Motoneurons were isolated from lumbar spinal cord of E14 C57/BL6 mice and plated at low density on laminin-111. These cell culture conditions allow minimal cell–cell contact and maximal axon extension of the cultured motoneurons (26). At DIV 7, motoneurons were stained with α-Tau antibody (Fig. 1A and B) and the axon length was measured (Fig. 1C and D). Motoneurons treated with 1–10 nM STX showed a significant decrease in the axon length (Fig. 1A and C). In contrast, TTX was not effective at the same low concentrations. The reduced axon length was observed only at TTX concentration of 50 nM (Fig. 1B and D) and higher (data not shown). Neither STX nor TTX had an influence on motoneuron survival at the same concentrations that led to the reduced axon growth (Fig. 1E and F). The number and length of motoneuron dendrites (Fig. 1G) were not affected when motoneurons were treated with 10 nM TTX or 10 nM STX (Fig. 1H and I).

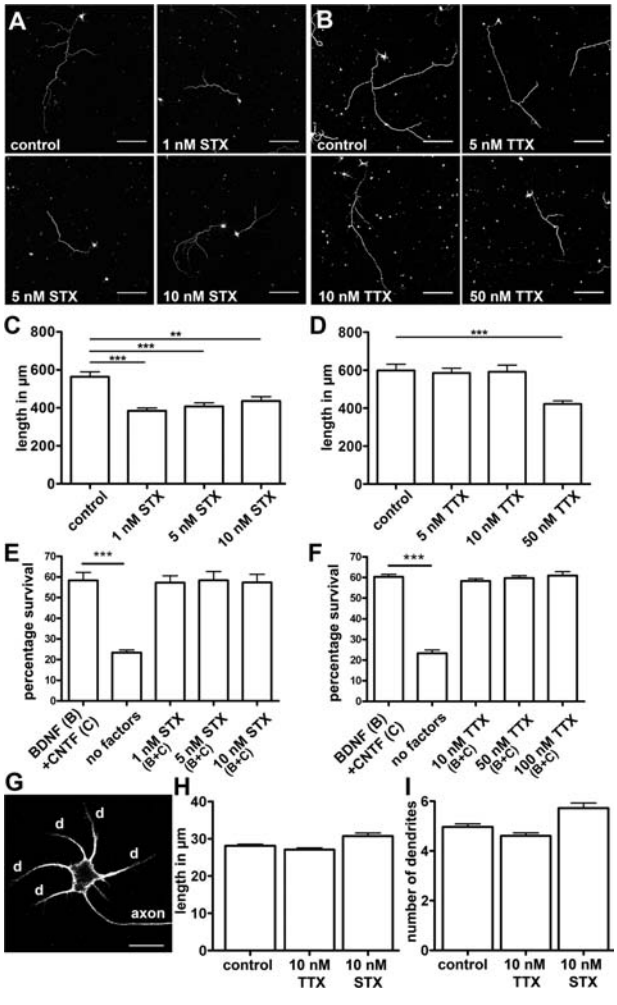

Figure 1. The axon elongation is reduced by pore blockers of VGSCs. (**A** and **B**) Axon length analysis of cultured motoneurons after anti-Tau staining. Analyzed cells were grown in the presence of saxitoxin (STX) and tetrodotoxin (TTX). (**C** and **D**) The axon length of motoneurons at indicated conditions. STX: 1 nM ($n = 168$), 5 nM ($n = 190$), 10 nM ($n = 185$) and TTX: 5 nM ($n = 158$), 10 nM ($n = 110$), 50 nM ($n = 140$). $Control_{STX\ treatments}$ $n = 183$, $control_{TTX\ treatments}$: $n = 101$. Bar (A–D): 150 µm. (**E** and **F**) Motoneuron survival in the presence or absence of neurotrophic factors, at indicated concentrations of STX and TTX ($n = 3$ independent cultures). (**G**) Dendrite analysis after anti-Tau staining. Bar: 15 µm. The dendrite length (**H**) and number of dendrites (**I**) of cultured motoneurons treated with or without STX (10 nM) and TTX (10 nM) values. Dendritic length: control, $n = 1182$; 10 nM TTX, $n = 976$; 10 nM STX, $n = 501$; number of dendrites, control, $n = 230$; 10 nM TTX, $n = 205$; 10 nM STX, $n = 81$. Results represent the mean ± SEM of pooled data from three independent experiments, *n*, number of motoneurons that were scored in total from control or toxin treated motoneurons. $^{***}P < 0.0001$; $^{**}P < 0.01$ tested by one-way ANOVA, Bonferroni *post hoc* test.

VGSC trigger spontaneous Ca^{2+} transients in cultured motoneurons

In cultured motoneurons, the axon growth is slow in a first phase until DIV 3, reaching about 100–150 μm of length. After DIV 3, axons grow fast, and they reach an average length of 600–800 μm at DIV 7. The frequency of local Ca^{2+} transients in axonal growth cones correlates with the speed of axon elongation during these different time periods in culture (17). To analyze the role of VGSCs in spontaneous excitability of motoneurons, we measured spontaneous Ca^{2+} transients with the calcium indicator dye Oregon-green BAPTA-1-AM (K_d: 130 nM) between DIV 3 and DIV 4, when the speed of axon elongation is highest. Initial experiments at DIV 3 showed that motoneurons were heterogeneous with respect to spontaneous activity, some showing low activity with rare Ca^{2+} transients and others with four or even more spontaneous transients per minute (not shown). Motoneurons can switch between such activity states (not shown). As suggested previously (15,27), we term broad spontaneous activity that results in synchronous transients in all parts of the cell as 'global activity', while locally restricted Ca^{2+} transients are termed 'local activity'. An example for such global activity is presented in Figure 2A and Supplementary Material, Movie S1, showing synchronous transients in three regions of interest (roi), namely the axon initiation segment (roi1), the axon (roi2) and the axonal growth cone (roi3). Figure 2B and Supplementary Material, movie S2 show an example for a motoneuron exhibiting spontaneous, local Ca^{2+} transients in the axon (roi2–4). The somatodendritic region was silent (roi1) when these Ca^{2+} transients were measured in the same cell.

From previous studies (17) we know that spontaneous Ca^{2+} influx to motoneurons is blocked by Ω-conotoxin. In accordance with this, 30 nM Ω-conotoxin MVIIa fully blocked spontaneous Ca^{2+} transients (Fig. 2C1 and C2). Ω-Conotoxin MVIIa has a high affinity to N-type VGCCs, while much higher concentrations lead to a block of other VGCCs (28). We then tested the sodium-channel pore blockers TTX and STX to figure out whether the opening of VGSCs triggers Ca^{2+} influx through VGCCs in motoneurons (Fig. 2D and E, Fig. 3). Low concentrations of STX (10 nM) had a strong inhibitory function on spontaneous Ca^{2+} influx (Figs 2D and 3B). TTX was less effective at 10 nM (Figs 2E and 3C), but showed a strong block of spontaneous activity when used at 100 nM (Fig. 3A and D). For quantitative analysis of VGSC function in triggering spontaneous Ca^{2+} transients, we analyzed motoneurons in the active state and monitored Ca^{2+} transients during a period of 40–60 min (long-term example is shown in Fig. 3A). Then, we analyzed transients in intervals (i) before the sodium-channel blocker treatment (Fig. 3A; spontaneous), (ii) in the presence of either STX or TTX, (iii) during the wash out of the channel blockers and (iv) 10 min after STX or TTX treatment, when activity recovers (spontaneous recovery) from toxin treatment (Fig. 3A). Spontaneous Ca^{2+} transients (Fig. 3B) were blocked by 10 nM STX in all cellular regions (soma, distal axon and growth cone), whereas TTX was less efficient to block these transients at the same concentration (Fig. 3C), in particular in the axon and axonal growth cone. The concentration of TTX necessary for an almost complete blockage of spontaneous Ca^{2+} transients was 100 nM (Fig. 3A and D). The effect was reversible when the inhibitors were washed out by a 10-fold artificial cerebrospinal fluid (ACSF) exchange (volume/min) over a period of 10 min. The experiments show that sodium-channel inhibitors reduce global and local Ca^{2+} transients in all cellular regions of motoneurons. Thus, the observation that low concentrations of STX inhibit axon elongation (Fig. 1) correlates with a reduced rate of Ca^{2+} transients under acute STX application.

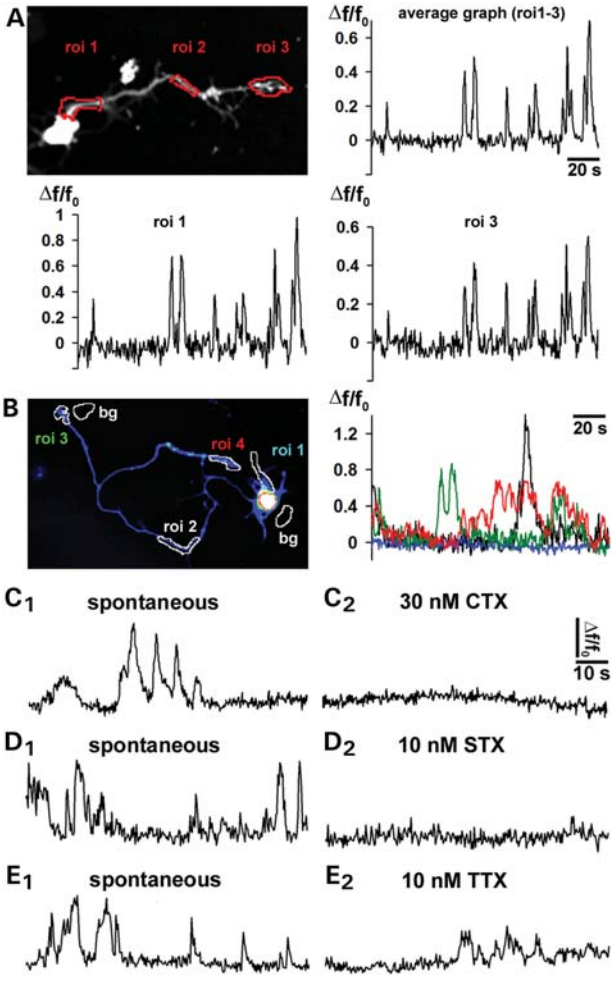

Figure 2. Characteristics of spontaneous calcium transients in motoneurons. (**A**) Representative motoneuron at DIV3 is loaded with the calcium indicator Oregon green BAPTA1-AM (left upper panel) and shows synchronous spontaneous global activity in three roi (roi1–3). (Right upper panel) Average change in fluorescence intensity ($\Delta f/f_0$) in roi1–3. (**B**) Motoneuron (in rainbow pseudocolor) with local activity in growth cones (roi3 green line and roi4, red line) and the axon (roi2, black line). The somatodendritic area in roi1 (blue line) did not show an increase in fluorescence during this imaging period. Spontaneous Ca^{2+} transients (**C_1**, **D_1**, **E_1**) are reduced by 30 nM Ω-CTX MVIIa (**C_2**), 10 nM STX (**D_2**), while 10 nM TTX (**E_2**) is less effective.

$Na_V1.9$ is expressed in cultured motoneurons

To identify the VGSCs that are responsible for triggering Ca^{2+} transients in developing motoneurons, we concentrated on $Na_V1.9$. Several lines of evidence point to $Na_V1.9$ as the

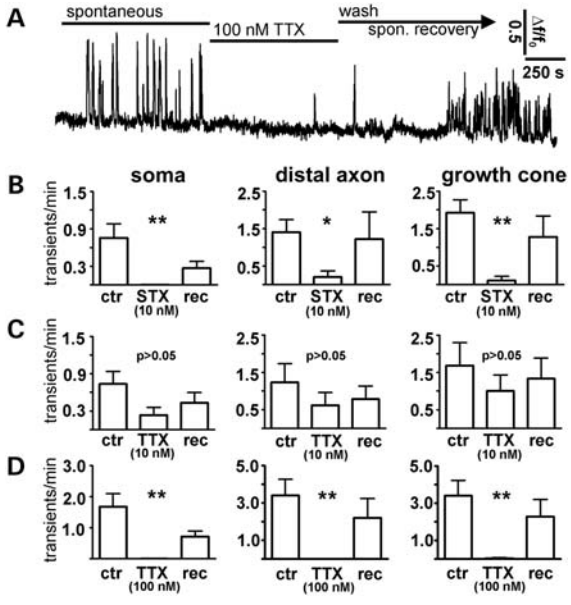

Figure 3. Spontaneous calcium transients in motoneurons are reduced by low concentrations of VGSC inhibitors. (**A**) Long-term imaging (4800 images at 2 Hz) of spontaneous activity in the growth cone of a cultured motoneuron, the block of spontaneous Ca^{2+} transients with 100 nM TTX and recovery of spontaneous activity by washing cells with ACSF under fast perfusion (10-fold buffer exchange per minute). (**B**) Frequency of spontaneous Ca^{2+} transients (transients/min) were determined at DIV 3, before toxin treatment (ctr), in the presence or absence of 10 nM STX ($n = 12$, **C**), 10 nM TTX ($n = 11$, **D**) and 10 min after ACSF perfusion wash, during the phase of recovery of spontaneous activity. Ca^{2+} transients were counted in the somatodendritic area, the distal axon and in growth cones. The number of local spontaneous Ca^{2+} transients is higher in growth cones compared with somatodendritic areas. 10 nM STX and 100 nM TTX block spontaneous activity in all cellular regions. Results represent the mean ± SEM of pooled data. $Cultures_{10nM\ STX} = 5$, $cultures_{10nM\ TTX} = 4$. $^{***}P < 0.0001$, $^{**}P < 0.01$, $^{*}P < 0.05$ tested by one-way ANOVA-nonparametric Kruskal–Wallis test, Dunn's post test.

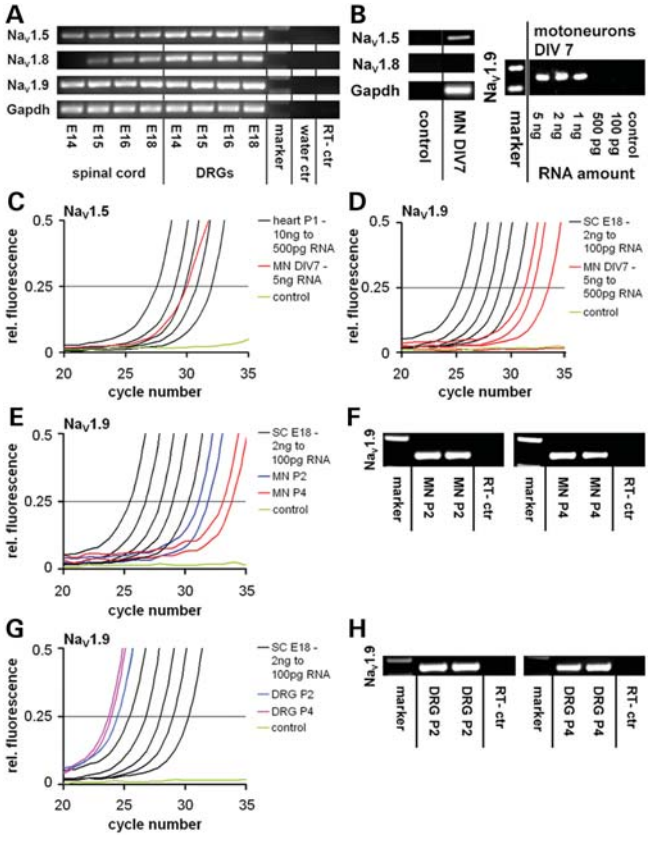

Figure 4. Early expression of $Na_V1.9$ in the spinal cord, DRG, cultured embryonic motoneurons and spinal cord motoneurons *in situ*. (**A**) Early expression of transcripts encoding for TTX-resistant VGSCs in the spinal cord and DRGs. Shown are representative amplification products after quantitative real-time RT–PCR with indicated cDNA sample material. The number of VGSC transcripts per RNA or per number of GAPDH transcripts was determined (see Table 1). (**B**) At DIV 7, transcripts encoding $Na_V1.9$ (right panel) 26 copies per 10 ng RNA; 0.11% of the amount of GAPDH and $Na_V1.5$ (left panel) are expressed in cultured motoneurons. $Na_V1.8$ was not detected (left panel). (**C** and **D**) Real-time monitoring of the fluorescence emission of Sybr Green1 during PCR amplification of $Na_V1.5$ (C) and $Na_V1.9$ (D). (**E** and **F**) $Na_V1.9$ expression in motoneurons and DRG neurons *in situ*. Real-time amplification curves of $Na_V1.9$ cDNA from laser-dissected motoneurons of the spinal cord (E) or DRG neurons (**G**) and corresponding $Na_V1.9$-specific amplification products (F and **H**). In $Na_V1.9$ amplification, serial dilutions of spinal cord RNA served as external control (black lines in D, E, G); for $Na_V1.5$, heart RNA was used as control (black lines, C).

most likely candidate for initiating VGSC-dependent spontaneous Ca^{2+} fluxes through VGCCs. $Na_V1.9$ has a low activation threshold and is able to mediate spontaneous excitation at resting potential levels, as shown previously in dorsal root ganglia (DRGs) and myenteric sensory neurons (29–32).

We therefore amplified transcripts encoding the TTX-resistant VGSCs $Na_V1.5$, $Na_V1.8$, and $Na_V1.9$ by efficiency-controlled quantitative RT–PCR (qRT–PCR) and determined the number of $Na_V1.9$ transcripts in the developing spinal cord, in DRGs and cultured motoneurons (Fig. 4A–D). In Fig. 4, representative amplification products and real-time PCR amplification curves are shown. For $Na_V1.9$ amplification, external standard dilution curves with E18 spinal cord RNA, 2 ng–100 pg, served as reference. $Na_V1.5$ is prominent for its function in triggering action potentials in the heart (24). Therefore, the heart RNA was used to produce $Na_V1.5$-specific external standard curves (10 ng–500 pg heart RNA). $Na_V1.9$ transcripts were detectable at E14 in spinal cord (8 copies/10 ng RNA) and DRG (70 copies/10 ng RNA). $Na_V1.9$ expression increased continuously between E14 and E18 (E18; spinal cord: 163 copies/10 ng RNA; DRG: 11 580 copies/10 ng RNA; Table 1; $n = 3$ independent experiments). In motoneuron cultures, substantial expression of $Na_V1.9$ (Fig. 4B, right panel) and $Na_V1.5$ transcripts (Fig. 4B, left panel) was found at DIV 7 whereas $Na_V1.8$ was not detectable (Fig. 4B). As the amplification efficiency of both gene-specific qRT–PCR protocols was almost identical ($eff_{Nav1.8} = 1.92$; $eff_{Nav1.9} = 1.95$), we conclude that $Na_V1.9$ mRNA is expressed at relatively high levels in motoneurons in comparison to $Na_V1.8$, which was below the detection limit. Interestingly, relative expression of $Na_V1.5$ was at least 27-fold higher than the expression of $Na_V1.9$. However, the activation threshold of $Na_V1.9$ is lower than that of $Na_V1.5$ (24), thus making it less likely that $Na_V1.5$ is upstream of $Na_V1.9$ in spontaneous excitation of motoneurons.

To reveal expression of $Na_V1.9$ in spinal motoneurons *in situ*, we microdissected motoneurons from spinal cord by laser capture microscopy at postnatal day 2 (P2), a time point that corresponds to the age of motoneurons that had been isolated at E14 and maintained in culture for 7 days

Table 1. Absolute quantification of $Na_V1.9$ transcripts

Origin of RNA	Spinal cord						DRG						MN
Developmental state	E12	E14	E15	E16	E18	P1	E12	E14	E15	E16	E18	P19	DIV7
Copies $Na_V1.9$/10 ng RNA	2	8	48	92	373	207	18	70	3499	4965	11 580	27 015	26
Copies $Na_V1.9$/copy GAPDH × 100	0.007	0.02	0.2	0.18	0.7	0.43	0.04	0.12	11.79	15.39	56.03	72.8	0.11

until they were analyzed. In addition, motoneurons were analyzed at P4. DRG neurons served as reference and GAPDH as denominator in all samples. As shown in Figure 4E and F, the spinal cord motoneurons express $Na_V1.9$ transcript at P2. In P2 motoneurons *in situ*, the number of $Na_V1.9$ transcripts is 0.44% of GAPDH transcripts, while in DRG neurons, 35 copies of $Na_V1.9$ correspond to 100 copies of GAPDH. Expression in motoneurons then decreases until P4 ($Na_V1.9$ versus GAPDH; 0.13%; Fig. 4E). At that stage, the relative expression of $Na_V1.9$ molecules versus GAPDH molecules in DRG neurons (Fig. 4G and H) is much higher than that in motoneurons.

Anti-$Na_V1.9$ antibody and identification of mouse $Na_V1.9$ protein in tissue

To detect $Na_V1.9$ protein in cultured motoneurons, anti-mouse $Na_V1.9$ antibodies were raised in rabbits. The C-terminal end of mouse $Na_V1.9$ was used for immunization (Fig. 5A). For control experiments, full-length mouse $Na_V1.9$ was cloned into a modified pcDNA3 vector and served as control. The rabbit antiserum [$Na_V1.9$ (71n)] that was raised against the C-terminus of the protein gave high titer antibodies and labeled recombinant human and mouse $Na_V1.9$ in western blots (Fig. 5B). Recombinant $Na_V1.9$ appeared in two bands with a relative molecular weight (M_r) of ~180 and ~280 kDa. The human $Na_V1.9$ protein was preferentially detected at ~280 kDa, as described earlier (33). When GFP and $Na_V1.9$ were co-expressed in HEK293 cells, $Na_V1.9$ immunoreactivity (ImmR) was specific to GFP+ cells (Fig. 5C). By increasing amounts of peptide used for immunization, $Na_V1.9$ (71n) ImmR was suppressed (Fig. 5C). Next, we established a stable HEK293T cell line expressing mouse $Na_V1.9$. Here, $Na_V1.9$ (71n) ImmR showed a distinct overlap with ImmR obtained with a pan-VGSC antibody (pan $Na_V1.x$) (Fig. 5D). Because $Na_V1.9$ is highly expressed in DRG neurons (Fig. 4), we used these neurons to detect endogenous $Na_V1.9$ protein. Endogenous $mNa_V1.9$ also showed an M_r of 180 and 280 kDa in western blots of lumbar and thoracic DRGs, while posterior nerve roots were $Na_V1.9$ negative in this experiment (Fig. 5E). Next, we prepared protein lysates of DRGs from $Na_V1.9^{-/-}$ mice. In this specific $Na_V1.9^{-/-}$ mouse line, a frameshift mutation introduces stop codons within exon 6 (31). In western blots from $Na_V1.9^{-/-}$ mice, $Na_V1.9$ ImmR is lost at an M_r of 180 and 280 kDa in DRGs from $Na_V1.9^{-/-}$ mice (Fig. 5F).

$Na_V1.9$ protein is localized in axons and axonal growth cones

To localize $Na_V1.9$ in cultured motoneurons, we used stimulated emission depletion (STED) microscopy and combined this technique with standard confocal laser scanning microscopy for the detection of F-Actin and α-Tubulin as structural markers. $Na_V1.9$ protein was not homogenously distributed in axons. When cultured motoneurons were stained with anti-$Na_V1.9$, ImmR was detectable along the axon but the staining appeared to be enriched at some sites (arrows in Fig. 6A and B). In axons and growth cones, $Na_V1.9$ ImmR was high in the distal axons and also found in small protrusions (right arrow in Fig. 6C). Single confocal STED planes revealed that small punctate anti-$Na_V1.9$ ImmR was lining along the cell surface of growth cones (arrows in Fig. 6D, upper and lower panel).

$Na_V1.9$ depletion reduces axon elongation

To test the role of $Na_V1.9$ for axon elongation, lentiviral shRNA expression vectors were designed and used to suppress the expression of this channel in motoneurons. The fluorescent protein Tandem-tomato (TDtomato) was co-expressed as infection control (Fig. 7). As a control for the efficacy of repression, shRNA-mediated $Na_V1.9$ knockdown was verified by western blot analysis of HEK293T cells expressing mouse $Na_V1.9$ (Fig. 7A; sh 63; sh 3028). $Na_V1.9$ expression was not reduced in cells expressing empty lentiviral vectors or constructs expressing missense control shRNA (mis 63) in which four bases were exchanged (Fig. 7A; sh vector, mis 63). Then, lentiviral vectors were used to infect motoneurons at DIV 1. Infected motoneurons were identified at DIV 7 and the axon length was analyzed. In sh 63-RNA-treated motoneurons, the axon length was reduced by 43% in comparison to uninfected motoneurons in the same cultures or control cultures treated with missense shRNA-expressing virus (Fig. 7B, red). A second set of lentivirally applied shRNA against the 3′-untranslated region of $Na_V1.9$, with GFP as infection control, showed 46% reduction in axon elongation in motoneurons at DIV 7 (Fig. 7B, green). Figure 7C shows representative motoneurons infected with lentiviral shRNA expression vectors expressing TDtomato as infection control. To address the question whether sh 63 was also effective on stably expressed $Na_V1.9$, a stable $Na_V1.9$ expressing-HEK293T cell line was transfected with control vector, sh 63 vector and a mis 63 shRNA. As shown in Figure 7D, shRNA expression but not mismatch shRNA reduced Nav1.9 expression to 18% compared with the control situation (Fig. 7E).

Motoneurons from $Na_V1.9^{-/-}$ mice exhibit shorter axons and reduced frequency of Ca^{2+} transients

We also isolated motoneurons from *$Na_V1.9$* knockout mice (31) and investigated them in comparison to strain-matched wild-type controls. No anti-$Na_V1.9$ ImmR was observed in motoneurons at DIV 5 (Fig. 8A). $Na_V1.9^{-/-}$ motoneurons

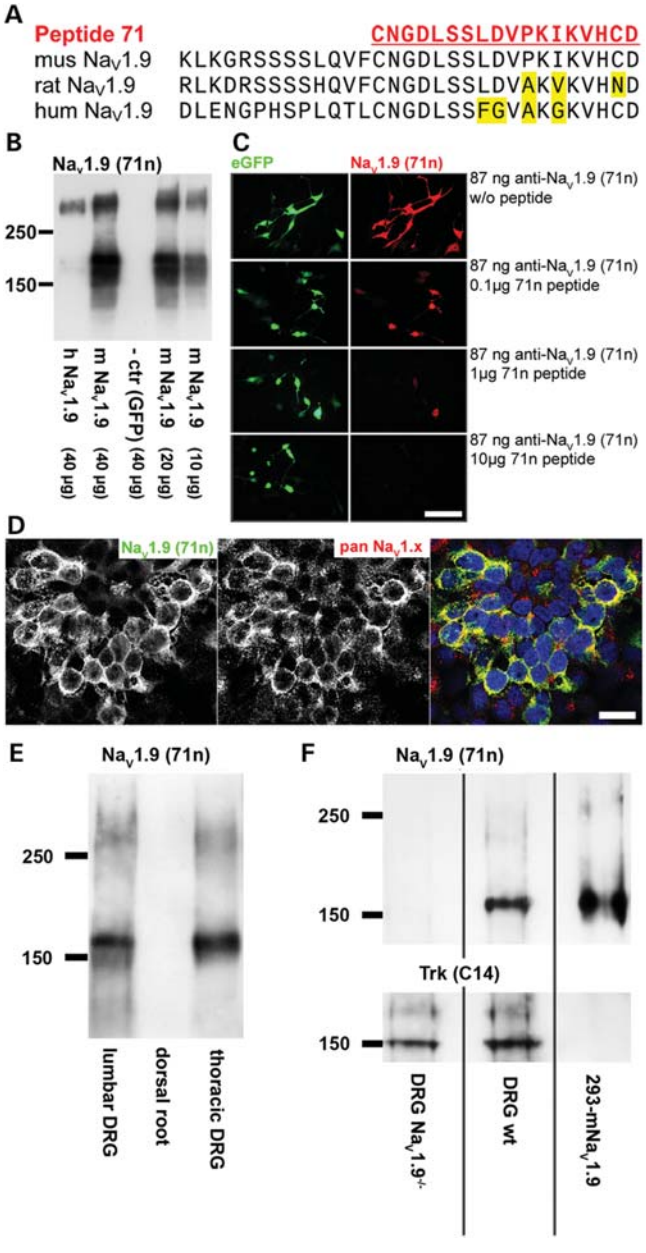

Figure 5. Anti-mouse Na$_V$1.9 antibody. (**A**) A peptide was deduced from the carboxyterminal end of mouse Na$_V$1.9 (red) and used for immunization of rabbits. The selected peptide sequence is specific for Na$_V$1.9. Differences to rat or human Na$_V$1.9 are marked (yellow). (**B**) Anti-Na$_V$1.9 (71n) recognizes recombinant human Na$_V$1.9 and mouse Na$_V$1.9 in western blot analysis. As vector control, GFP-expressing vectors were used. (**C**) Immunoreactivity of anti-Na$_V$1.9 (71n) on recombinant Na$_V$1.9 is blocked by the corresponding 71n immunization peptide. Bar: 100 µm (**D**) Stable expression of mNa$_V$1.9 in HEK293T cells reveals a pronounced overlap of anti-Na$_V$1.9 (71n) and anti-pan Na$_V$1.x immunoreactivity. Bar: 15 µm. (**E**) Endogenous mouse Na$_V$1.9 from lumbar and thoracic DRGs is displayed by two bands at M_r 180 kDa and ~280 kDa. (**F**) Endogenous mouse Na$_V$1.9 in wild-type DRGs and recombinant Na$_V$1.9 in the stable cell line 293-mNa$_V$1.9 are displayed by the typical double-band pattern bands at M_r 180 kDa and ~280 kDa. Both bands are lost in Na$_V$1.9$^{-/-}$ mice (representative for $n = 4$). Anti-Trk (*tropomyosin*-related-kinase) antibodies served as loading control for DRG tissue.

showed highly reduced rates of spontaneous Ca^{2+} transients at DIV 3, in the soma (−75%), distal axonal regions (−82%) and growth cones (−83%) (Fig. 8B), indicating that the loss of Na$_V$1.9 affects global and local Ca^{2+} transients of spontaneous excitability. Dendritic elongation (Fig. 8C) and motoneuron survival (Fig. 8D) were unaffected. However, axon elongation of *Na$_V$1.9*$^{-/-}$ motoneurons was reduced by 38% compared with wild-type littermates (Fig. 8E).

We then investigated whether the reduction of spontaneous Ca^{2+} transients observed in motoneurons from a mouse model of SMA (*Smn*$^{-/-}$*/SMN2*) (17) is also influenced by inhibition of Na$_V$1.9 and other VGSCs. In *Smn*$^{-/-}$*/SMN2* mice, spontaneous Ca^{2+} transients are reduced because of defects in the clustering of the Ca$_V$2.2 in axon terminals thus leading to a reduced axonal elongation (17). When Smn$^{-/-}$/SMN2 motoneurons were treated with 10 nM STX, axonal elongation remained unchanged, showing that function-blocking concentrations of STX have no additional growth inhibiting effect on *Smn*$^{-/-}$*/SMN2* motoneurons (Fig. 8F). This experiment raised the question whether Na$_V$1.9 expression and protein distribution has changed in *Smn*$^{-/-}$*/SMN2* motoneurons. Immunolocalization of Na$_V$1.9 in *Smn*$^{-/-}$*/SMN2* motoneurons revealed Na$_V$1.9 concentration in axons and axon terminals (Fig. 9A, four representative distal axons and growth cones are shown). Next, we performed qPCR on RNA samples harvested from four independent single-embryo motoneuron cultures of *Smn*$^{-/-}$*/SMN2* motoneurons. Expression levels of Na$_V$1.9 at DIV 7 in *Smn*$^{-/-}$*/SMN2* motoneurons are comparable in control and *SMN*-deficient motoneurons (Fig. 9B and C).

DISCUSSION

Spontaneous activity plays an important role during development of the nervous system when neurons make connections and synaptic networks are shaped (10,11,13–16). During development, motoneurons become spontaneously active long before they make synaptic contacts with skeletal muscle (9,16,34). In culture, embryonic mouse motoneurons display spontaneous Ca^{2+} transients that are important for axon elongation and growth cone differentiation (17). Downstream Ca^{2+}-dependent signaling pathways modulate microfilament and microtubule networks that mediate the effects of spontaneous excitability on the axon growth (35). Blockade of VGCC by Ω-conotoxin leads to ~40% reduced axon elongation in cultured embryonic mouse motoneurons on laminin-111 (17), indicating that depolarization-induced Ca^{2+} influx plays a major role in axon elongation.

Here, we provide evidence that the VGSC Na$_V$1.9 acts as an upstream trigger of spontaneous excitatory Ca^{2+} influx in motoneurons and thus modulates the rate of axon elongation, without affecting motoneuron survival. Apparently, other members of the Na$_V$ family cannot compensate for the deficiency of Na$_V$1.9. This is not unexpected. Among the nine members of the Na$_V$1 family, Na$_V$1.9 exhibits a specific property in that it opens spontaneously when neurons are kept close to the resting potential (29–32). The effect on axon elongation

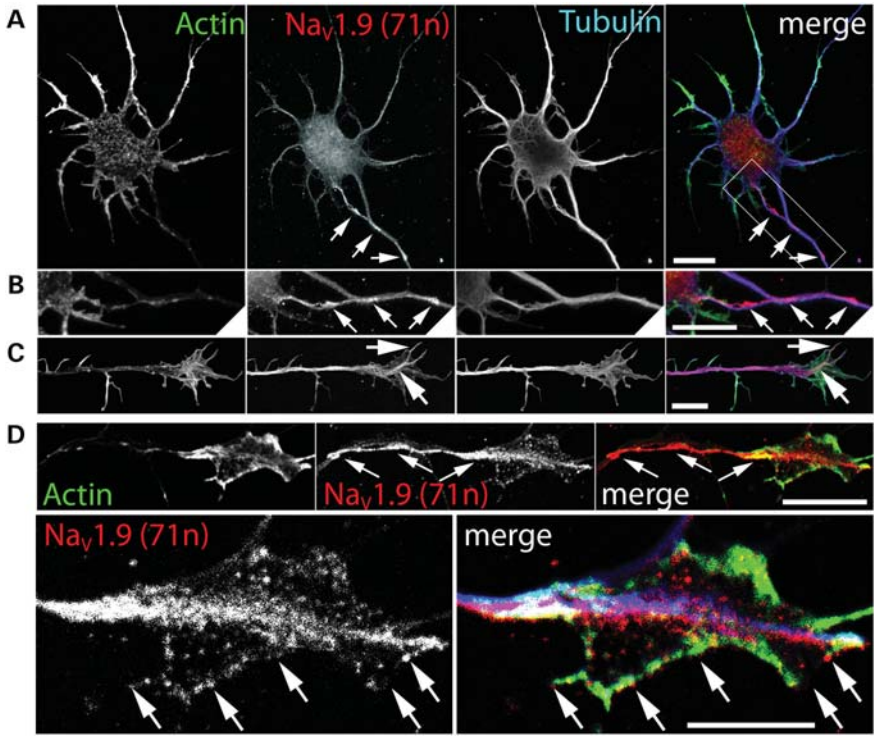

Figure 6. $Na_v1.9$ protein in cultured motoneurons. (**A**–**D**) Single confocal sections of anti-$Na_V1.9$ staining of motoneurons by STED microscopy, combined with standard laser scanning microscopy of Actin and α-Tubulin staining. (A) Arrows point to anti-mouse $Na_V1.9$ immunoreactivity (ImmR), concentrated in axonal regions of cultured motoneurons (DIV 7). The inlet is enlarged in (B). (B) In the axon, $Na_V1.9$ protein is detectable along the axon, but the staining appeared to be enriched at some sites (arrows). (C) Example of a growth cone at DIV 3, where anti-$Na_V1.9$ ImmR (arrows) is found in fine protrusions (right arrow) of the growth cone. Bar (in A–C): 10 μm. (D, upper panel) Example of a motoneuron growth cone at DIV 7. $Na_V1.9$ is concentrated in axonal region and then found on the surface (arrows) of the growth cone in small punctate-like elements, as revealed by STED microscopy. Bar: 10 μm (D, lower panel). Magnification of the growth cone shown in the upper panel. In the merge image, Actin is shown in green and α-tubulin staining is blue. Arrows point to $Na_V1.9$ ImmR at the cell surface. Bar: 5 μm.

observed in motoneurons from *$Na_V1.9$* knockout mice and in motoneurons in which $Na_V1.9$ is acutely suppressed by shRNA was similar. This argues against the possibility that deficiency of $Na_V1.9$ in knockout mice leads to a developmental defect that indirectly impairs spontaneous activity. Furthermore, the blockage of voltage-gated Na^+ channels by STX and, at least at higher concentrations, that by TTX provokes a similar extent in the reduction of spontaneous activity and axon elongation. This appears remarkable as TTX and STX should act on a broad spectrum of VGSCs, and the reduction in spontaneous activity and axon elongation observed with these pharmacological inhibitors is not higher than after $Na_V1.9$ knockout or shRNA-mediated knockdown. This indicates that $Na_V1.9$ is the predominant VGSC that triggers spontaneous activity for axon elongation. Spontaneous Ca^{2+} transients in embryonic motoneurons are either locally restricted or globally distributed over the whole cell. In *$Na_V1.9^{-/-}$* motoneurons, Ca^{2+} transients are massively reduced at DIV 3–4, both global transients that are synchronously observed in all parts of the cell and local transients that are seen only in axons.

Voltage-gated Ca^{2+} influx modulates the axon growth in motoneurons that are cultured at low-density so that the cells cannot make synaptic contact with each other. Furthermore, during the monitoring of Ca^{2+} influx, cells were kept under fast perfusion in an ACSF extracellular solution with 3 mM potassium. These characteristics would hardly allow motoneuron depolarization with ligand-dependent stimuli by synaptic input or excitatory neurotransmitters in the medium.

$Na_V1.9$ is responsible for prolonged sodium influx into a variety of neurons (29,31,33,36,37) and thus can depolarize the cells so that Ca^{2+} influx through VGCCs can occur with high efficacy. Moreover, $Na_V1.9$ is predominantly localized in axons and axonal growth cones so that opening of VGCCs by $Na_V1.9$ is facilitated even under conditions when opening of $Na_V1.9$ provokes only a local depolarization in axonal growth cones. In embryonic chick motoneurons, a persistent sodium current is involved in the generation of spontaneous excitatory bursts (13) and experiments by Kastenenka and Landmesser have demonstrated that spinal motor circuits are sensitive to the precise frequency and pattern of spontaneous activity (38). The molecular identity of the persistent sodium current which is involved in normal firing patterns of chick motoneurons has not been identified and it is tempting to speculate that $Na_V1.9$ plays a central role. As chick $Na_V1.9$ (NM_001192868) is 79% identical with mouse $Na_V1.9$ (NM_011887), it may be possible that $Na_V1.9$ is the upstream trigger of spontaneous Ca^{2+} bursts during motoneuron pathfinding in the chick.

A critical issue is how the opening of $Na_V1.9$ is regulated. Studies on fast (milliseconds) excitatory transients after brain-derived neurotrophic factor (BDNF) application (39)

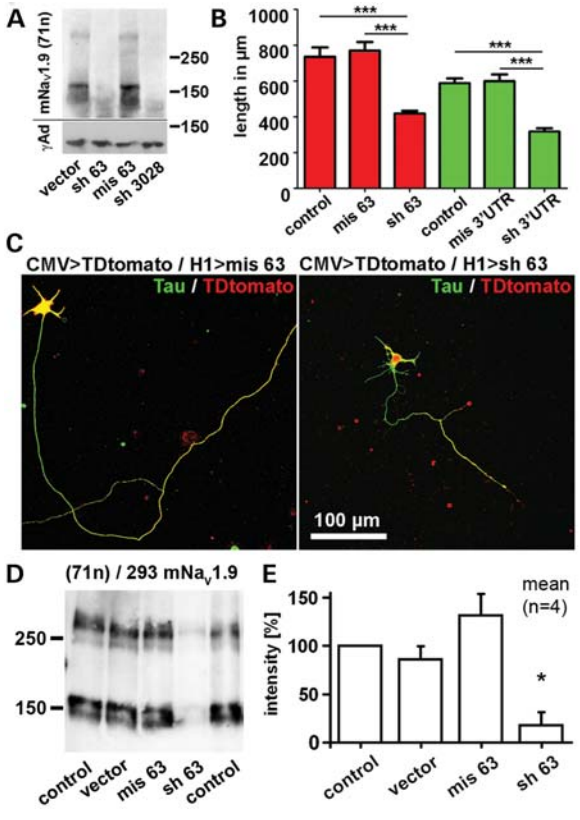

Figure 7. $Na_V1.9$ regulates axon elongation of cultured motoneurons. (**A**) Knockdown of recombinant mouse $Na_V1.9$ by shRNA (sh 63, sh 3028), but not missense shRNA (mis 63) or empty sh-expression vector (sh vector). Western blot analysis after transient transfection in HEK293T cells using anti-$Na_V1.9$ (71n). Loading control: γ-Adaptin (γAd). (**B**) Axon length analysis after lentiviral shRNA expression. Red bars: lentiviral construct with cytomegalovirus (CMV)-TDtomato-H1-shRNA: uninfected ($n = 67$), mis 63 $Na_V1.9$ ($n = 108$), sh 63 $Na_V1.9$ ($n = 105$). Green bars: U6-shRNA-CMV-eGFP: uninfected ($n = 134$), mis 3′ UTR $Na_V1.9$ ($n = 65$), sh 3′ UTR $Na_V1.9$ ($n = 65$). Results represent the mean ± SEM of pooled data from three independent experiments, *n*, number of motoneurons. $^{***}P < 0.0001$ tested by one-way ANOVA-nonparametric Kruskal–Wallis test, Dunn's post test. (**C**) Representative motoneurons infected with a missense shRNA expression construct (pSIH-TDtomato-mis 63-shRNA; left panel) or $Na_V1.9$ knockdown construct (pSIH-TDtomato-sh 63-shRNA; right panel). Shown are merged confocal images with anti-Tau immunolabel (green) and TDtomato signals (red). TDtomato signals were amplified by anti-RFP immunostaining. (**D**) Western blot analysis of $Na_V1.9$ after transient transfection of shRNA expression vectors and control vectors in a HEK293T cell line with stable expression of mouse $Na_V1.9$. (**E**) Mean intensity (in %) of anti-m$Na_V1.9$ western blot stainings (as in D) under shRNA knockdown or corresponding control conditions (mean ± SEM, $n = 4$ independent experiments; $^{*}P < 0.05$ tested by one-way ANOVA-nonparametric Kruskal–Wallis test, Dunn's post test).

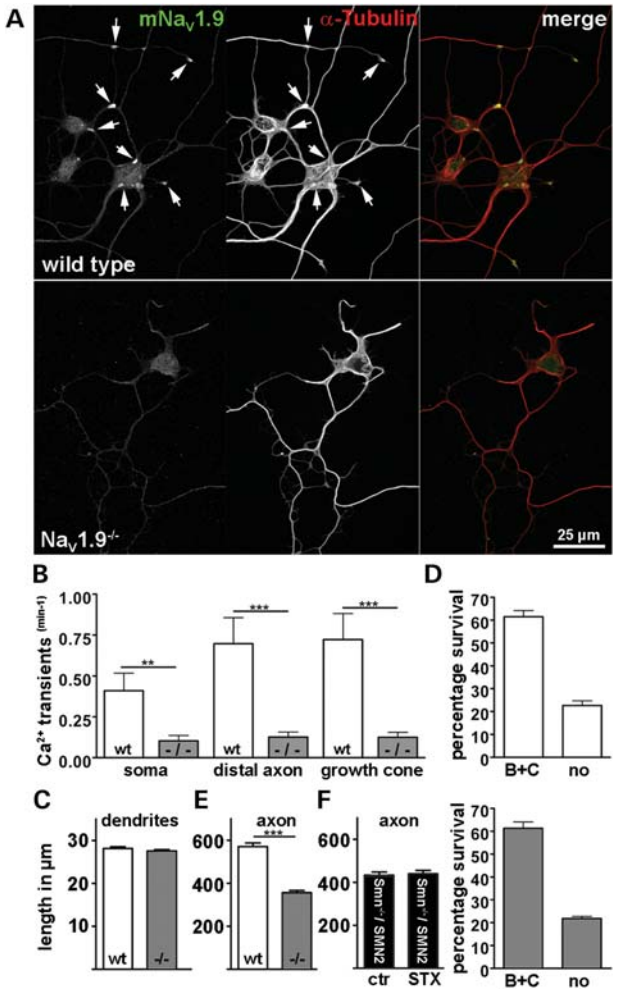

Figure 8. Reduced axon growth and less spontaneous Ca^{2+} transients in motoneurons from $Na_V1.9^{-/-}$ mice. (**A**) $Na_V1.9$ (71n) antiserum reveals lack of $Na_V1.9$ protein (arrows upper panel) in motoneurons (DIV 5) of $Na_V1.9^{-/-}$ mice (lower panel). (**B**) Spontaneous Ca^{2+} transients are reduced in the soma, distal axon and growth cone of motoneurons cultured from $Na_V1.9^{-/-}$ mice (+/+: $n = 80$; $Na_V1.9^{-/-}$: $n = 138$; four independent cultures). (**C**) The dendrite length is unaffected in $Na_V1.9^{-/-}$ motoneurons (+/+: $n = 752$ dendrites; $Na_V1.9^{-/-}$: $n = 1049$ dendrites; three independent cultures). (**D**) Motoneuron survival in the presence of the neurotrophic factors BDNF and ciliary neurotrophic factor (B and C) is not disturbed in $Na_V1.9^{-/-}$ motoneurons ($n = 2$ independent cultures). (**E**) The axon elongation is reduced in $Na_V1.9^{-/-}$ motoneurons (+/+: $n = 286$; $Na_V1.9^{-/-}$: $n = 447$; 3 independent cultures). (**F**) Axonal elongation of motoneurons of $Smn^{-/-}/SMN2$ mice is not reduced by 10 nM STX treatment (ctr: $n = 197$, mean length: 433 µm; 10 nM STX: $n = 241$, mean length: 439 µm; $n = 3$ coverslips). $^{***}P < 0.001$; $^{**}P < 0.01$ tested by two-tailed nonparametric Mann–Withney test.

suggested that $Na_V1.9$ can be opened in central neurons by BDNF via TrkB activation (33,40). However, the existence of such BDNF–induced fast Na^+ currents has become controversial (41). In particular, it has been noted that the kinetics of BDNF release conflict with the much faster activation kinetics of the $Na_V1.9$–mediated currents (42). The motoneurons used in our study were continuously cultured with BDNF to support their survival. Thus, it is possible that TrkB signaling is involved in the cascades that lead to opening of VGCCs (43) through $Na_V1.9$. It is unlikely that Ca^{2+} elevation in motoneurons is caused by spontaneously released BDNF from cells in these cultures, given that BDNF is present at concentrations of 10 ng/ml that saturate TrkB receptors on the cell surface. However, it is possible that other signaling mechanisms such as transactivation of TrkB receptors (44) that are not exposed on the cell surface contributes to the opening probability of $Na_V1.9$ (31,45) and therefore might increase the local, growth-mediating excitability of motoneurons. It is unresolved whether $Na_V1.9$ is opened by direct interaction with TrkB or indirectly via other signaling pathways or TrkB-dependent rapid changes in ion fluxes that alter the resting potential in such a way that $Na_V1.9$ can open.

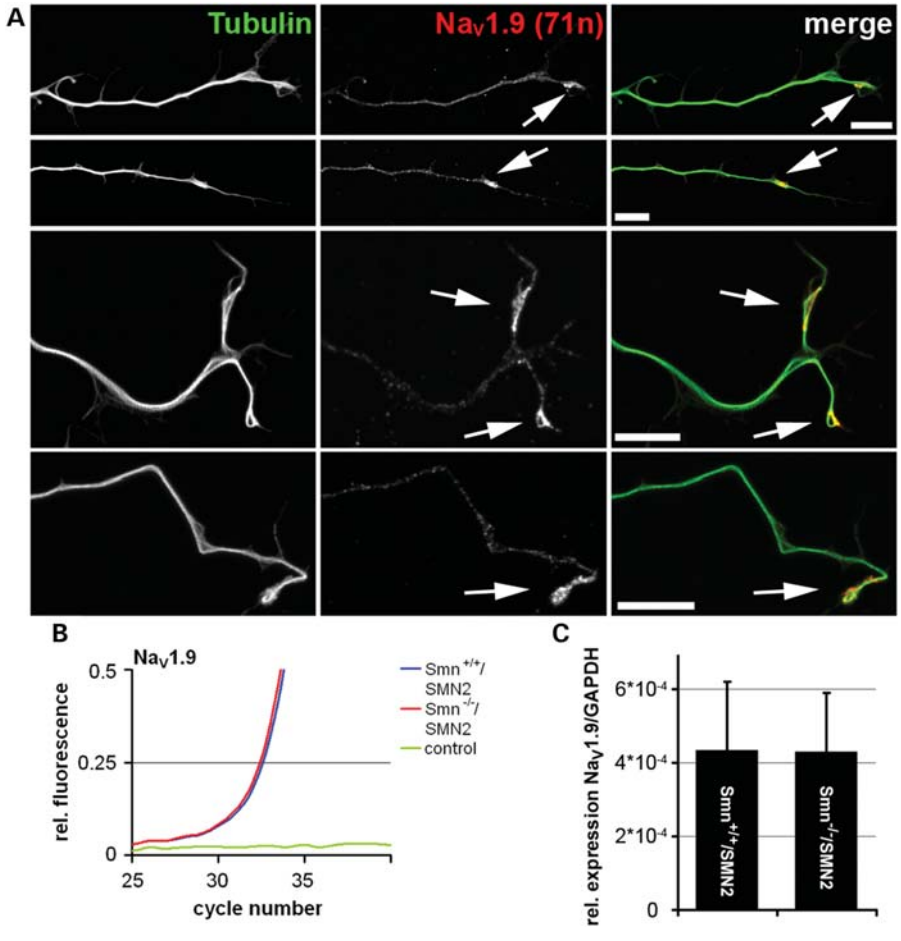

Figure 9. $Na_v1.9$ protein and $Na_V1.9$ expression levels in cultured *SMN*$^{-/-}$*/SMN2* motoneurons. (**A**) Single confocal sections of anti-$Na_V1.9$ staining of motoneurons by standard laser scanning microscopy of α-Tubulin staining. Arrows point to anti-mouse $Na_V1.9$ immunoreactivity (ImmR), concentrated in distal axonal regions and growth cones. Bar in all images: 10 μm. (**B**) Real-time monitoring of the fluorescence emission of Sybr Green1 during PCR amplification of $Na_V1.9$. Shown are the mean value curves of four independent motoneuron preparations, blue: *SMN*$^{+/+}$*/SMN2* cDNA was used; red: *SMN*$^{-/-}$*/SMN2*; green: control. (**C**) Relative expression levels of $Na_V1.9$ in comparison to GAPDH (efficiency corrected). Shown are mean values ($n = 4$) ± SD.

The apparent effect of $Na_V1.9$ on axon elongation in cultured embryonic motoneurons appears to be not reflected by the relatively mild phenotype of $Na_V1.9$ knockout mice (31,46,47). These mice develop normally, and show only defects in pain perception, but no apparent functional defect that is caused by a reduced axon growth of motoneurons to reach their target, the skeletal muscles (46). This is not surprising when the effects of $Na_V1.9$ knockout are compared with models for SMA in which Smn expression is reduced. Isolated motoneurons from a mouse model of SMA (48) show severe defects in Ca^{2+} transients in axons and axonal growth cones, and the reduced frequency of Ca^{2+} transients also correlates with a reduced axon elongation (17). However, the axons of the Smn-deficient motoneurons reach skeletal muscle, and no reduction in neuromuscular endplate formation is observed in mouse embryos with Smn deficiency (49,50). However, when Smn (51) or Smn-interacting proteins such as hnRNPR (52) are knocked down by Morpholino technologies in zebrafish, the axons of motoneurons show severe defects in axon elongation and pathfinding. This indicates that animal models in which the motor axon growth occurs within a short time window suffer more from these genetic defects than developing mice in which axon elongation, pathfinding and synapse formation occur over a relatively prolonged time period. Thus, a failsafe mechanism seems to exist that compensates for the reduced speed of axon elongation and allows motoneurons to reach their target.

The signaling cascades leading to motoneuron differentiation and motoneuron axon elongation are also of central interest for the development of therapies for motoneuron diseases, in particular SMA in which a defect in synapse maintenance appears as a central pathophysiological mechanism (17,48–50,53). Previous studies indicate that intracellular signaling pathways can activate persistent sodium currents by $Na_V1.9$ (31,45). This raises the hope that pharmacological activation to increase the opening probability of $Na_V1.9$ could be a way to stimulate axon regeneration and maintenance.

MATERIALS AND METHODS

Animals

All experimental procedures were done in accordance with European Union guidelines, as approved by our institutional

animal care and utilization committee. The following mouse lines were used in this study: C57BL/6J mice; *$Na_V1.9^{-/-}$* mice on a C57BL/6J background (31) and *$Smn^{-/-}$/SMN2* mice (48) on a FVB/NCrl background.

Cell culture

Spinal motoneurons were isolated from 14-day-old C57/BL6/J mouse embryos of either sex, enriched by panning using an antibody against the $p75^{NTR}$ receptor and plated at a density of 1500 cells/well on laminin-coated coverslips as described previously (26). Cells were grown in neurobasal medium containing B27 supplement, 10% heat inactivated horse serum, 500 μM Glutamax (Invitrogen), 10 ng/ml BDNF and 10 ng/ml ciliary neurotrophic factor. Medium was replaced after 24 h and then every second day. Ω-Conotoxins MVIIa (Sigma), tetrodotoxin (Sigma, Ascent Scientific) and saxitoxin (Sigma) was added at indicated concentrations. Motoneuron survival was determined after 7 days in culture as described earlier (54). Motoneurons from $Na_V1.9$ or Smn/SMN2 mouse models were prepared from single embryos. Genotyping was then performed from corresponding tissue samples.

Quantitative real-time reverse transcriptase–polymerase chain reaction

Reverse transcription, primer selection and qPCR were performed with minor modifications as described in earlier studies (55–57). RNA from mouse embryonic DRG and the spinal cord was isolated by standard protocols using RNeasy Plus-Mini-Kit (Qiagen), with the help of a silent crusher (Heidolph). RNA from single-embryo motoneuron cultures (Smn/SMN2 RNA samples) was prepared with the RNeasy Micro Kit (Qiagen). qPCRs were run on a Lightcycler 1.5 (Roche) using FastStart DNA master SYBR green1 reagents, using kinetic PCR cycles. Offline analysis to calculate efficiency-controlled relative expression levels or absolute copy numbers was carried out according to Rasmussen (58). Intron-spanning primers were selected with Oligo 6.0 software (MedProbe) and PCR conditions, primer concentration and $MgCl_2$ concentration were optimized as described (55). Reactions were performed in glass capillaries in a volume of 20 μl. PCR products were analyzed by gel electrophoresis, melting curve analysis and control PCRs. Primers and PCR targets: $mNa_V1.9$ (AF118044): 1992-for 5′-CCCTTGTGAGTCTC GCTGAC-3′; 2114-rev 5′-GGAGTGGCCGATGATCTTA AT-3′; 143 bp, intron-spanning. $mNa_V1.8$ (NM_009134): 25 41-for 5′-CATTCCTTCCTCGTCGTC-3′; 2676-rev 5′-AAA GCGATGAATAGGTTGAG-3′, 155 bp, intron-spanning. $mNa_V1.5$ (NM_021544): 712-for 5′-TTCACCGCCATCTA CACCT-3′; 855-rev 5′-GAGCCGACAAATTGCCTAGC-3′; 163 bp, intron-spanning. GAPDH (NM_008084): 205-for 5′-GCAAATTCAACGGCACA-3′; 337-rev 5′-CACCAGTAG ACTCCACGAC-3′; 141 bp, pseudo-genes. β-Actin (NM_007393): for 5′-GCCAACCGTGAAAAGATGAC-3′; rev 5′GGCGTGAGGGAGAGCATAG-3′. Kinetic cycle conditions in four segments: $mNa_V1.9$ (95°C, 0 s, 59°C, 5 s, 72°C, 6 s, 83°C, 5 s), 2 mM $MgCl_2$, 30 pmol primer; efficiency (55). $mNa_V1.8$ (95°C, 0 s, 58°C, 5 s, 72°C, 7 s, 85°C, 5 s) 2 mM $MgCl_2$, 30 pmol primer. $mNa_V1.5$ (95°C, 0 s, 59°C, 5 s, 72°C, 7 s, 85°C, 5 s) 2 mM $MgCl_2$, 50 pmol primer. GAPDH (95°C, 0 s, 59°C, 5 s, 72°C, 6 s, 83°C, 5 s) 3 mM $MgCl_2$, 30 pmol primer, efficiency: 2.00. β-Actin (95°C, 10 s, 55°C, 10 s, 72°C, 5 s, 86°C, 5 s) 2 mM $MgCl_2$, 10 pmol primer.

Laser capture microdissection

Laser capture microdissection (Leica DM6000B laser microdissection system) was used to isolate motoneurons from the spinal cord of 2- and 4-day-old postnatal mice. In addition, DRG neurons, which express high numbers of $Na_V1.9$ transcripts, were collected as reference. Spinal cord sections were embedded in optimum cutting temperature compound (Tissue-Tek) and immediately immersed in isopentane, chilled in liquid nitrogen for rapid freezing. Cross-sections of 15 μm thickness were prepared on a Leica cryostat, transferred to 0.9 μm POL membranes (Leica) and stained in Cresyl Violet solution. A total of 500–1200 MN cell bodies were collected in RNA lysis buffer. Total RNA was purified from the samples (59) and real-time RT–PCR was performed (see above). To compare expression levels of $Na_V1.9$ in motoneurons versus DRG neurons, GAPDH expression served as denominator and relative expression was calculated.

Cloning of mouse $Na_V1.9$, shRNA expression vectors

For stable propagation in *E. coli*, the rop-element of pBR322 was introduced to the backbone of pcDNA3 as described earlier (33). Next, mouse $Na_V1.9$ was cloned from mouse brain mRNA by fusing three partial cDNA PCR fragments. An artificial Kozak sequence (CCACCATG) was introduced before the start codon. The resulting construct was sequenced on both strands. Expression was tested by western blot analysis and immunocytochemistry using antibodies against $Na_V1.9$ (71n) and pan-$Na_V1.X$ (Sigma, clone K58/35, 1–2 ng/ml). For lentiviral expression of shRNA targeted against $Na_V1.9$ transcripts and shRNA missense controls, two series of vectors were used. Sequences were selected (60) and cloned to the vector LL3.7 (61). In this case, shRNA was directed against the 3′ UTR of $Na_V1.9$ and expressed under U6 promoter. GFP expressed under cytomegalovirus (CMV) promoter served as infection control. In a second set basing on pSIH-H1 (System Biosciences), we replaced CMV-driven copGFP against TDTomato (62) and expressed shRNA against the coding region of $Na_V1.9$ and corresponding missense control shRNA under H1 promoter. To test the shRNA performance, $mNa_V1.9$ expression backbone (A.W., S.H. and R.B., in preparation) was mixed with shRNA expression vectors, transfected to HEK293T cells and co-expressed for 72 h. Then cells were lysed and $Na_V1.9$ protein was visualized by western blot analysis. In a second set of experiments, shRNA expression vectors were transfected to a cell with stable expression of $mNa_V1.9$ and quantitative analysis of shRNA efficiency was determined by western blot analysis.

Antibody production: anti-mouse $Na_V1.9$ (71n)

First, pre-immune serum was tested by immunofluorescence and western blot analysis. Antibodies were raised in pre-tested

rabbits against the C-terminus of mouse $Na_V1.9$. As antigen, a keyhole limpet hemocyanin-coupled peptide (CNGDLSSLDVPKIKVHCD*) was used. Sera were tested after the fourth (71) and fifth boost (71n). Antibodies were affinity purified (immunization peptide on column) and stored in Tris–glycine, 250 mM NaCl, 1 mg/ml bovine serum albumin, 0.01% Thimerosal, 50% glycerol at −20°C at a final concentration of 400 μg/ml.

Detection of $Na_V1.9$ in HEK293T cells (recombinant) or DRGs (endogenous) using western blot analysis

DRGs were prepared from adult *Nav1.9*$^{-/-}$ mice and wild-type mice of either sex, separated from nerve roots and collected in phosphate-buffered saline (PBS) on ice. Four to six lumbar or 6–10 thoracic DRGs were homogenized in 90 μl of 2% NP40 (or Igepal), 150 mM NaCl, 50 mM Tris–HCl, 10 mM DTT (fresh), 10% glycerol including protease inhibitors (Roche) using a ultrasonic homogenizer (Hielscher UP50H with MS1 sonotrode). After a first round of a 10 s pulse with 100% amplitude, lysates were incubated on ice for 10 min and homogenized again under same conditions. An aliquot of 75 μl of the sample were mixed with 4× Laemmli SDS–PAGE loading buffer and incubated at 50°C for 10 min. HEK293T protein was prepared in 2% NP40 (or Igepal), 150 mM NaCl, 50 mM Tris–HCl, 10% glycerol including protease inhibitors (Roche). SDS–PAGE on $Na_V1.9$ was performed with Tris–Acetate gradient gels (4–7%; BioRad). Protein lysates (40–60 μg per lane) were blotted (semi-dry) on polyvinylidene difluoride membranes (BioRad), blocked with 5% milk powder (BioRad) and labeled with rabbit anti-$Na_v1.9$ (71n) (1:1000) and re-probed with mouse anti-human γ-adaptin (1:2000; Sigma, clone 100/3) for loading control. As loading control for DRG protein, anti-Trk (C14, Santa Cruz, 0.2 μg/ml) was used. Antibodies were detected using ECL-detection reagents (GE Healthcare).

Lentivirus production

In HEK293T cells, pSIH-H1-based lentiviral vectors were packaged with pCMV-VSVG and pCMVΔR8.91 (63) as described earlier (64). shRNA expressing pLL3.7 was packaged with pRSV Rev, pMDLg/pRRE and pMD.G (65,66). Vectors were transfected with Lipofectamine 2000 (Invitrogen) in OptiMEM medium with 10% fetal calf serum for 12–14 h and viral supernatants were harvested 72 h after transfection. Lentiviral particles were concentrated from cleared supernatants by two rounds of ultracentrifugation at 25 000 rpm in a Beckman SW28 rotor for 2 h at 4°C. The virus pellet was soaked on ice for a minimum of 4 h in 200 μl tris-buffered saline buffer (in mM): 130 NaCl, 10 KCl, 5 $MgCl_2$ and 50 Tris–HCl, pH 7.8. Aliquots (10 μl) of the viral suspension were stored at −80°C. Titering was performed on HeLa cells and 10^5 infectious particles were used to infect 5 000 freshly prepared E14 motoneurons in suspension before plating.

Immunocytochemistry

Cultures were fixed in 4% PBS-buffered paraformaldehyde at 37°C for 10–20 min. Blocking and permeabilization was performed in 1× PBS, 10% BSA, 0.05–0.1% Triton X-100, 0.1% Tween 20, pH 7.4, for 1 h. For visualization of $Na_V1.9$ in axons, 0.3% Triton X-100 was used. Primary antibodies were incubated in blocking solution for 3 h at room temperature. The following antibodies were used: rabbit anti-Tau (Sigma, 1/1000); mouse anti-Map2 (clone AP-20, Sigma, 1/400); pan-anti-Sodium channel ($Na_V1.x$; Sigma clone K58/35, 1/500); mouse anti-Tubulin (Sigma, clone B-5-1-2, 1/2000). In washing steps, 1× PBS, 0.1% Triton X-100, 0.1% Tween 20 was used. Samples were detected by secondary antibodies labeled with Alexa 488 (Invitrogen), Dylight 488, Cy3, or Cy5 (Jackson Immunoresearch). Nuclei were labeled by DAPI (400 pg ml^{-1}) in PBS. Actin was labeled with Alexa Fluor-546 phalloidin (Invitrogen). Cells were embedded in Aqua Polymount (Polysciences) and monitored using Leica confocal systems (TCS SP series) equipped with Leica objectives (HC PL Apo ×20/0.7; HCX Apo ×40/1.25–0.75 oil, ×60/1.4–0.6 oil).

STED microscopy

STED microscopy was performed on a Leica SP5 confocal laser scanning microscope equipped with a Mai-Tai multi photon laser (Spectra-Physics). m$Na_V1.9$ (71n) immunoreactivity (ImmR) was detected with anti-rabbit Atto647N secondary antibodies. A Leica HCX PL Apo CS ×100/1.4 oil objective was used for the STED detection. Serial scanning of anti-Tubulin and phalloidin ImmR was performed by standard confocal imaging. Images were taken at 12-bit, in single confocal planes.

Axon length analysis

The axon length was determined by applying a morphometric system (Leica, Bensheim, Germany) on confocal image material.

Confocal Ca^{2+} imaging

A 5 mM stock solution of Oregon green-BAPTA1-AM (Invitrogen; O6807) was prepared in 8.9 μl of 20% Pluronic F-127 (Invitrogen) in dimethyl sulfoxide by means of a sonifier bath (Bandelin) for 2 min. Motoneurons were incubated with 5 μM Oregon green-BAPTA1-AM in ACSF solution. Motoneurons were loaded with dye-containing ACSF in a cell culture incubator (37°C, 5% CO_2) for 10–15 min. Motoneurons were imaged at an inverted confocal microscope (Leica SP series) using a ×20/0.7 objective under continuous perfusion in a low chamber volume (∼200 μl) with high buffer exchange rate (∼10× chamber volume per min, in some experiments: ∼20× volume exchange/min). Ligands (Sigma, Ascent Scientific) were used at the following concentrations: tetrodotoxin (TTX; 100–10 nM) and saxitoxin (STX; 100–10 nM). In some cases, muscimol (10–50 μM); or γ-aminobutyric acid (GABA) (100 μM) were used as control stimulus to monitor the excitatory action of GABA on embryonic motoneurons. Time lapse monitoring (256 × 256 pixel) of Ca^{2+} dynamics was performed at 2.0 Hz. Oregon green-BAPTA1-derived fluorescence was excited with a 488 nm laser line (emission detection: 507/565 nm). For pharmacological effect of VGSC inhibitors on spontaneous Ca^{2+} transients in motoneurons, cells were analyzed in their active state, under conditions of activity block

and in a phase of the recovery of activity after pharmacological treatment (Fig. 3). In case of $Na_V1.9^{-/-}$ motoneurons and strain-matched control cells (Fig. 8), all cells in the field of interest were analyzed. ACSF contained (in mM): 127 NaCl, 3 KCl, 2.5 NaH_2PO_4, 2 $CaCl_2$, 2 $MgCl_2$, 23 $NaHCO_3$ and 25 D-glucose, bubbled with 95% O_2/5% CO_2.

Image analysis

Images were analyzed using ImageJ software (WS Rasband, ImageJ, US National Institutes of Health, Bethesda, MD, USA, http://rsb.info.nih.gov/ij/, 1997–2006) and processed with Photoshop (Adobe Systems, San Jose, CA, USA). XY-time Ca^{2+} imaging results were analyzed by a roi analysis (pixel intensity; $\Delta f/f_0$ analysis).

SUPPLEMENTARY MATERIAL

Supplementary Material is available at *HMG* online.

ACKNOWLEDGEMENTS

We are grateful to Hilde Troll, Regine Sendtner, Nicole Elflein and Michaela Keßler for excellent technical assistance and Mike Friedrich for introduction in STED microscopy. $Na_V1.9^{-/-}$ mice were kindly provided by John Wood, London.

Conflict of Interest statement. None declared.

AUTHORS' CONTRIBUTIONS

R.B., M.S. designed research; N.S., A.W., B.D., P.Y., S.H., S.J., R.B. performed research; M.A.N. contributed analytic tools; N.S., A.W., B.D., P.Y., S.J. and R.B. analyzed data; R.B. and M.S. wrote the paper.

FUNDING

This work was supported by grants from the Deutsche Forschungsgemeinschaft, BL567 and SFB581, project B1 and B24 and the from the Hermann und Lilly Schilling Stiftung im Stifterverband der Deutschen Wissenschaft. P.Y. was supported by a grant of the German Excellence Initiative to the Graduate School of Life Sciences, University of Würzburg.

REFERENCES

1. Sanes, J.R. and Lichtman, J.W. (1999) Development of the vertebrate neuromuscular junction. *Annu. Rev. Neurosci.*, **22**, 389–442.
2. Hamburger, V. (1934) The effects of wing bud extirpation on the development of the central nervous system in chick embryos. *J. Exp. Zool.*, **68**, 449–494.
3. Hamburger, V. (1975) Cell death in the development of the lateral motor column of the chick embryo. *J. Comp. Neurol.*, **160**, 535–546.
4. Thoenen, H., Hughes, R.A. and Sendtner, M. (1993) Trophic support of motoneurons: physiological, pathophysiological, and therapeutic implications. *Exp. Neurol.*, **124**, 47–55.
5. Arakawa, Y., Sendtner, M. and Thoenen, H. (1990) Survival effect of ciliary neurotrophic factor (CNTF) on chick embryonic motoneurons in culture: comparison with other neurotrophic factors and cytokines. *J. Neurosci.*, **10**, 3507–3515.
6. Calof, A.L. and Reichardt, L.F. (1984) Motoneurons purified by cell sorting respond to two distinct activities in myotube-conditioned medium. *Dev. Biol.*, **106**, 194–210.
7. Sendtner, M., Pei, G., Beck, M., Schweizer, U. and Wiese, S. (2000) Developmental motoneuron cell death and neurotrophic factors. *Cell Tissue Res.*, **301**, 71–84.
8. Hanson, M.G. and Landmesser, L.T. (2003) Characterization of the circuits that generate spontaneous episodes of activity in the early embryonic mouse spinal cord. *J. Neurosci.*, **23**, 587–600.
9. Nishimaru, H., Iizuka, M., Ozaki, S. and Kudo, N. (1996) Spontaneous motoneuronal activity mediated by glycine and GABA in the spinal cord of rat fetuses in vitro. *J. Physiol.*, **497**(Pt 1), 131–143.
10. O'Donovan, M.J. and Landmesser, L. (1987) The development of hindlimb motor activity studied in the isolated spinal cord of the chick embryo. *J. Neurosci.*, **7**, 3256–3264.
11. Spitzer, N.C. (2006) Electrical activity in early neuronal development. *Nature*, **444**, 707–712.
12. Ciccolini, F., Collins, T.J., Sudhoelter, J., Lipp, P., Berridge, M.J. and Bootman, M.D. (2003) Local and global spontaneous calcium events regulate neurite outgrowth and onset of GABAergic phenotype during neural precursor differentiation. *J. Neurosci.*, **23**, 103–111.
13. Wang, S., Polo-Parada, L. and Landmesser, L.T. (2009) Characterization of rhythmic Ca^{2+} transients in early embryonic chick motoneurons: Ca^{2+} sources and effects of altered activation of transmitter receptors. *J. Neurosci.*, **29**, 15232–15244.
14. Spitzer, N.C., Lautermilch, N.J., Smith, R.D. and Gomez, T.M. (2000) Coding of neuronal differentiation by calcium transients. *Bioessays*, **22**, 811–817.
15. Gu, X. and Spitzer, N.C. (1995) Distinct aspects of neuronal differentiation encoded by frequency of spontaneous Ca^{2+} transients. *Nature*, **375**, 784–787.
16. Hanson, M.G. and Landmesser, L.T. (2004) Normal patterns of spontaneous activity are required for correct motor axon guidance and the expression of specific guidance molecules. *Neuron*, **43**, 687–701.
17. Jablonka, S., Beck, M., Lechner, B.D., Mayer, C. and Sendtner, M. (2007) Defective Ca^{2+} channel clustering in axon terminals disturbs excitability in motoneurons in spinal muscular atrophy. *J. Cell Biol.*, **179**, 139–149.
18. Chan, Y.B., Miguel-Aliaga, I., Franks, C., Thomas, N., Trulzsch, B., Sattelle, D.B., Davies, K.E. and van den Heuvel, M. (2003) Neuromuscular defects in a *Drosophila* survival motor neuron gene mutant. *Hum. Mol. Genet.*, **12**, 1367–1376.
19. Kong, L., Wang, X., Choe, D.W., Polley, M., Burnett, B.G., Bosch-Marce, M., Griffin, J.W., Rich, M.M. and Sumner, C.J. (2009) Impaired synaptic vesicle release and immaturity of neuromuscular junctions in spinal muscular atrophy mice. *J. Neurosci.*, **29**, 842–851.
20. Ruiz, R., Casanas, J.J., Torres-Benito, L., Cano, R. and Tabares, L. (2010) Altered intracellular Ca^{2+} homeostasis in nerve terminals of severe spinal muscular atrophy mice. *J Neurosci*, **30**, 849–857.
21. Porter, B.E., Weis, J. and Sanes, J.R. (1995) A motoneuron-selective stop signal in the synaptic protein S-laminin. *Neuron*, **14**, 549–559.
22. Nishimune, H., Sanes, J.R. and Carlson, S.S. (2004) A synaptic laminin-calcium channel interaction organizes active zones in motor nerve terminals. *Nature*, **432**, 580–587.
23. Catterall, W.A. (2000) From ionic currents to molecular mechanisms: the structure and function of voltage-gated sodium channels. *Neuron*, **26**, 13–25.
24. Catterall, W.A., Goldin, A.L. and Waxman, S.G. (2005) International Union of Pharmacology. XLVII. Nomenclature and structure–function relationships of voltage-gated sodium channels. *Pharmacol. Rev.*, **57**, 397–409.
25. Penzotti, J.L., Fozzard, H.A., Lipkind, G.M. and Dudley, S.C. Jr. (1998) Differences in saxitoxin and tetrodotoxin binding revealed by mutagenesis of the Na_+ channel outer vestibule. *Biophys. J.*, **75**, 2647–2657.
26. Wiese, S., Herrmann, T., Drepper, C., Jablonka, S., Funk, N., Klausmeyer, A., Rogers, M.L., Rush, R. and Sendtner, M. (2010) Isolation and enrichment of embryonic mouse motoneurons from the lumbar spinal cord of individual mouse embryos. *Nat. Protoc.*, **5**, 31–38.
27. Gu, X., Olson, E.C. and Spitzer, N.C. (1994) Spontaneous neuronal calcium spikes and waves during early differentiation. *J. Neurosci.*, **14**, 6325–6335.

28. Feng, Z.P., Doering, C.J., Winkfein, R.J., Beedle, A.M., Spafford, J.D. and Zamponi, G.W. (2003) Determinants of inhibition of transiently expressed voltage-gated calcium channels by omega-conotoxins GVIA and MVIIA. *J. Biol. Chem.*, **278**, 20171–20178.
29. Cummins, T.R., Dib-Hajj, S.D., Black, J.A., Akopian, A.N., Wood, J.N. and Waxman, S.G. (1999) A novel persistent tetrodotoxin-resistant sodium current in SNS-null and wild-type small primary sensory neurons. *J. Neurosci.*, **19**, RC43.
30. Herzog, R.I., Cummins, T.R. and Waxman, S.G. (2001) Persistent TTX-resistant Na(+) current affects resting potential and response to depolarization in simulated spinal sensory neurons. *J. Neurophysiol.*, **86**, 1351–1364.
31. Östman, J.A., Nassar, M.A., Wood, J.N. and Baker, M.D. (2008) GTP up-regulated persistent Na^+ current and enhanced nociceptor excitability require NaV1.9. *J. Physiol.*, **586**, 1077–1087.
32. Rugiero, F., Mistry, M., Sage, D., Black, J.A., Waxman, S.G., Crest, M., Clerc, N., Delmas, P. and Gola, M. (2003) Selective expression of a persistent tetrodotoxin-resistant Na+ current and NaV1.9 subunit in myenteric sensory neurons. *J. Neurosci.*, **23**, 2715–2725.
33. Blum, R., Kafitz, K.W. and Konnerth, A. (2002) Neurotrophin-evoked depolarization requires the sodium channel Nav1.9. *Nature*, **419**, 687–693.
34. Milner, L.D. and Landmesser, L.T. (1999) Cholinergic and GABAergic inputs drive patterned spontaneous motoneuron activity before target contact. *J. Neurosci.*, **19**, 3007–3022.
35. Zhou, F.Q. and Snider, W.D. (2006) Intracellular control of developmental and regenerative axon growth. *Philos. Trans. R. Soc. Lond. B Biol. Sci*, **361**, 1575–1592.
36. Baker, M.D., Chandra, S.Y., Ding, Y., Waxman, S.G. and Wood, J.N. (2003) GTP-induced tetrodotoxin-resistant Na^+ current regulates excitability in mouse and rat small diameter sensory neurones. *J. Physiol.*, **548**, 373–382.
37. Coste, B., Osorio, N., Padilla, F., Crest, M. and Delmas, P. (2004) Gating and modulation of presumptive NaV1.9 channels in enteric and spinal sensory neurons. *Mol. Cell Neurosci.*, **26**, 123–134.
38. Kastanenka, K.V. and Landmesser, L.T. (2010) In vivo activation of channelrhodopsin-2 reveals that normal patterns of spontaneous activity are required for motoneuron guidance and maintenance of guidance molecules. *J. Neurosci.*, **30**, 10575–10585.
39. Kafitz, K.W., Rose, C.R., Thoenen, H. and Konnerth, A. (1999) Neurotrophin-evoked rapid excitation through TrkB receptors. *Nature*, **401**, 918–921.
40. Lang, S.B., Stein, V., Bonhoeffer, T. and Lohmann, C. (2007) Endogenous brain-derived neurotrophic factor triggers fast calcium transients at synapses in developing dendrites. *J. Neurosci.*, **27**, 1097–1105.
41. Minichiello, L. (2009) TrkB signalling pathways in LTP and learning. *Nat. Rev. Neurosci.*, **10**, 850–860.
42. Brigadski, T., Hartmann, M. and Lessmann, V. (2005) Differential vesicular targeting and time course of synaptic secretion of the mammalian neurotrophins. *J. Neurosci.*, **25**, 7601–7614.
43. Blum, R. and Konnerth, A. (2005) Neurotrophin-mediated rapid signaling in the central nervous system: mechanisms and functions. *Physiology (Bethesda)*, **20**, 70–78.
44. Wiese, S., Jablonka, S., Holtmann, B., Orel, N., Rajagopal, R., Chao, M.V. and Sendtner, M. (2007) Adenosine receptor A2A-R contributes to motoneuron survival by transactivating the tyrosine kinase receptor TrkB. *Proc. Natl. Acad. Sci. USA*, **104**, 17210–17215.
45. Rush, A.M. and Waxman, S.G. (2004) PGE2 increases the tetrodotoxin-resistant Nav1.9 sodium current in mouse DRG neurons via G-proteins. *Brain Res.*, **1023**, 264–271.
46. Leo, S., D'Hooge, R. and Meert, T. (2010) Exploring the role of nociceptor-specific sodium channels in pain transmission using Nav1.8 and Nav1.9 knockout mice. *Behav. Brain Res.*, **208**, 149–157.
47. Priest, B.T., Murphy, B.A., Lindia, J.A., Diaz, C., Abbadie, C., Ritter, A.M., Liberator, P., Iyer, L.M., Kash, S.F., Kohler, M.G. *et al.* (2005) Contribution of the tetrodotoxin-resistant voltage-gated sodium channel NaV1.9 to sensory transmission and nociceptive behavior. *Proc. Natl Acad. Sci. USA*, **102**, 9382–9387.
48. Monani, U.R., Sendtner, M., Coovert, D.D., Parsons, D.W., Andreassi, C., Le, T.T., Jablonka, S., Schrank, B., Rossoll, W., Prior, T.W. *et al.* (2000) The human centromeric survival motor neuron gene (SMN2) rescues embryonic lethality in Smn(−/−) mice and results in a mouse with spinal muscular atrophy. *Hum. Mol. Genet.*, **9**, 333–339.
49. McGovern, V.L., Gavrilina, T.O., Beattie, C.E. and Burghes, A.H. (2008) Embryonic motor axon development in the severe SMA mouse. *Hum. Mol. Genet.*, **17**, 2900–2909.
50. Murray, L.M., Lee, S., Bäumer, D., Parson, S.H., Talbot, K. and Gillingwater, T.H. (2010) Pre-symptomatic development of lower motor neuron connectivity in a mouse model of severe spinal muscular atrophy. *Hum. Mol. Genet.*, **19**, 420–433.
51. McWhorter, M.L., Monani, U.R., Burghes, A.H. and Beattie, C.E. (2003) Knockdown of the survival motor neuron (Smn) protein in zebrafish causes defects in motor axon outgrowth and pathfinding. *J. Cell Biol.*, **162**, 919–931.
52. Glinka, M., Herrmann, T., Funk, N., Havlicek, S., Rossoll, W., Winkler, C. and Sendtner, M. (2010) The heterogeneous nuclear ribonucleoprotein-R is necessary for axonal beta-actin mRNA translocation in spinal motor neurons. *Hum. Mol. Genet.*, **19**, 1951–1966.
53. Rossoll, W., Jablonka, S., Andreassi, C., Kroning, A.K., Karle, K., Monani, U.R. and Sendtner, M. (2003) Smn, the spinal muscular atrophy-determining gene product, modulates axon growth and localization of beta-actin mRNA in growth cones of motoneurons. *J. Cell Biol.*, **163**, 801–812.
54. Götz, R., Wiese, S., Takayama, S., Camarero, G.C., Rossoll, W., Schweizer, U., Troppmair, J., Jablonka, S., Holtmann, B., Reed, J.C. *et al.* (2005) Bag1 is essential for differentiation and survival of hematopoietic and neuronal cells. *Nat. Neurosci.*, **8**, 1169–1178.
55. Durand, G.M., Marandi, N., Herberger, S.D., Blum, R. and Konnerth, A. (2006) Quantitative single-cell RT-PCR and Ca^{2+} imaging in brain slices. *Pflugers Arch.*, **451**, 716–726.
56. Hartmann, J., Blum, R., Kovalchuk, Y., Adelsberger, H., Kuner, R., Durand, G.M., Miyata, M., Kano, M., Offermanns, S. and Konnerth, A. (2004) Distinct roles of Galpha(q) and Galpha11 for Purkinje cell signaling and motor behavior. *J. Neurosci.*, **24**, 5119–5130.
57. Rose, C.R., Blum, R., Pichler, B., Lepier, A., Kafitz, K.W. and Konnerth, A. (2003) Truncated TrkB-T1 mediates neurotrophin-evoked calcium signalling in glia cells. *Nature*, **426**, 74–78.
58. Rasmussen, R. (2001) Quantification on the LightCycler. In: Meurer, S., Wittwer, C. and Nakawara, K. (eds), *Rapid Cycle Real-Time PCR, Methods and Applications*. Springer, Berlin, Heidelberg, pp. 21–34.
59. Liss, B. (2002) Improved quantitative real-time RT-PCR for expression profiling of individual cells. *Nucleic Acids Res.*, **30**, e89.
60. Elbashir, S.M., Harborth, J., Lendeckel, W., Yalcin, A., Weber, K. and Tuschl, T. (2001) Duplexes of 21-nucleotide RNAs mediate RNA interference in cultured mammalian cells. *Nature*, **411**, 494–498.
61. Rubinson, D.A., Dillon, C.P., Kwiatkowski, A.V., Sievers, C., Yang, L., Kopinja, J., Rooney, D.L., Zhang, M., Ihrig, M.M., McManus, M.T. *et al.* (2003) A lentivirus-based system to functionally silence genes in primary mammalian cells, stem cells and transgenic mice by RNA interference. *Nat. Genet.*, **33**, 401–406.
62. Shaner, N.C., Campbell, R.E., Steinbach, P.A., Giepmans, B.N., Palmer, A.E. and Tsien, R.Y. (2004) Improved monomeric red, orange and yellow fluorescent proteins derived from *Discosoma* sp. red fluorescent protein. *Nat. Biotechnol.*, **22**, 1567–1572.
63. Zufferey, R., Nagy, D., Mandel, R.J., Naldini, L. and Trono, D. (1997) Multiply attenuated lentiviral vector achieves efficient gene delivery in vivo. *Nat. Biotechnol.*, **15**, 871–875.
64. Rehberg, M., Lepier, A., Solchenberger, B., Osten, P. and Blum, R. (2008) A new non-disruptive strategy to target calcium indicator dyes to the endoplasmic reticulum. *Cell Calcium*, **44**, 386–399.
65. Dull, T., Zufferey, R., Kelly, M., Mandel, R.J., Nguyen, M., Trono, D. and Naldini, L. (1998) A third-generation lentivirus vector with a conditional packaging system. *J. Virol.*, **72**, 8463–8471.
66. Naldini, L., Blomer, U., Gallay, P., Ory, D., Mulligan, R., Gage, F.H., Verma, I.M. and Trono, D. (1996) In vivo gene delivery and stable transduction of nondividing cells by a lentiviral vector. *Science*, **272**, 263–267.